



## NOTES AND CORRESPONDENCE

### A Four-Year Lidar–Sun Photometer Aerosol Study at São Paulo, Brazil

EDUARDO LANDULFO

*Instituto de Pesquisas Energéticas e Nucleares, São Paulo, Brazil*

ALEXANDROS PAPAYANNIS

*National Technical University of Athens, Zografou, Greece*

ANI SOBRAL TORRES, SANDRO TOSHIO UEHARA, LUCILA MARIA VIOLA POZZETTI, CAIO ALENCAR DE MATOS,  
PATRICIA SAWAMURA, WALTER MORINOBU NAKAEMA, AND WELLINGTON DE JESUS

*Instituto de Pesquisas Energéticas e Nucleares, São Paulo, Brazil*

(Manuscript received 24 January 2007, in final form 29 November 2007)

#### ABSTRACT

A backscattering lidar system, the first of this kind in Brazil, has been used to provide the vertical profile of the aerosol backscatter coefficient at 532 nm up to an altitude of 4–6 km above sea level (ASL), in a suburban area in the city of São Paulo. The lidar system has been operational since September 2001. The lidar data products were obtained in a 4-yr period (2001–04) and concerned the aerosol optical thickness (AOT), the aerosol backscattering and extinction coefficients at 532 nm, cloud properties (cloud base, thickness), planetary boundary layer (PBL) heights, aerosol layering, and the structure and dynamics of the lower troposphere. The lidar data are presented and analyzed in synergy with AOT measurements obtained by a Cimel sun-tracking photometer in the visible spectral region, not only to validate the lidar data but also to provide an input value of the so-called extinction-to-backscatter ratio [lidar ratio (LR)]. A correlation between the lidar data and the data obtained by a Cimel sun-tracking photometer [belonging to the Aerosol Robotic Network (AERONET)] is being made to set a temporal database of those data that were collected concomitantly and to cross correlate the information gathered by each instrument. The sun photometer data are used to provide AOT values at selected wavelengths and thus to derive the Ångström exponent (AE) values, single scattering albedo (SSA) and phase function values, and LR values. The analysis of these data showed an important trend in the seasonal signature of the LR indicating a change of the predominant type of aerosol between the dry and wet seasons. Thus, during the wet season the LR lidar values are greater (50–60 sr), which indicates that larger absorption by the aerosols takes place during this period. The corresponding AE values range between 1.3 and 2 for both periods.

#### 1. Introduction

Air pollution in megacities is one of the most important problems of our era. The city of São Paulo, Brazil, ranks as one of the five largest metropolitan areas of the world, as well as one of the most populated areas (about 11 million inhabitants). In all these megacities,

human activities have an enormous impact on the quality of the local atmosphere, as well as on the population's health. Concerning the atmospheric quality, we highlight the high concentrations of the suspended aerosol particles as a subject of continuous interest because of the ongoing expansion of the metropolitan area, which carries over 15 000 industries. The study of aerosols in such an environment is not only crucial but very important in assessing the local and regional impact on climate and population health. Aerosol data from these geographical locations in the Southern Hemisphere are not as abundant as in Europe, North

---

*Corresponding author address:* Eduardo Landulfo, IPEN, Av. Prof. Lineu Prestes, 2242, Cidade Universitária, São Paulo, SP-05508-000 Brazil.  
E-mail: elandulf@ipen.br

America, and northern Asia. Among the several means to measure the aerosols parameters we highlight the ground-based remote sensing, in particular the lidar and sun photometric techniques.

The lidar technique is based on the emission of a collimated laser beam in the atmosphere and on the detection of the backscattered laser light by the suspended atmospheric aerosols and atmospheric molecules. The lidar technique, through its high temporal (from seconds to minutes) and spatial (3–15 m) resolution, is a powerful tool to visualize in real time the structure of the PBL using the aerosols as passive tracers of the atmospheric dynamic processes. The sun photometer data are used to provide the aerosol optical thickness (AOT) values at selected wavelengths and thus, to derive the Ångström exponent (AE) values. The synergy of Cimel and lidar measurements also acts to minimize the uncertainties of the assumptions made, especially when inverting the lidar signal using Klett's technique (Klett 1985).

In Brazil, a continent-sized country, there are only two operating lidar systems; the first one is devoted to stratospheric studies (Clemesha and Rodrigues 1971) and the second one, an elastic backscatter lidar system, is devoted to tropospheric aerosol profiling for air pollution applications (Landulfo et al. 2004).

The synergy of ancillary meteorological measurements and simultaneous investigations of the optical properties of the suspended aerosols (by sun photometers or spectrophotometers) can provide additional information for reducing the lidar data retrieval errors (aerosol extinction and backscatter profiles). Especially, this synergy of measurements helps to minimize the uncertainties of the assumptions made when inverting the lidar signals (Takamura et al. 1994) using the input value of the extinction-to-backscatter ratio [lidar ratio (LR)], since it is well known that the lidar ratio has a wide range of values that depend on the relative humidity (RH) and on the origin of the air masses sampled (Anderson et al. 2000; Ackermann 1998). Recently, a variability study of the lidar ratio was made by Cattrall et al. (2005) emphasizing its climatology in the face of 26 different locations of the globe.

In this paper we present a statistical analysis of the aerosol optical properties retrieved over the city of São Paulo, using the synergy of lidar and sun photometer measurements performed concomitantly between the years 2001 and 2004. We first compare the lidar ratios retrieved by the Aerosol Robotic Network (AERONET) products ("cloud free" level-1.5 data) available in São Paulo with the ones obtained by lidar, through tuning of the lidar data to match the AOT values given by the Cimel photometer (Landulfo et al. 2003). The

lidar ratio variability is presented and the presence of a seasonal signature is evaluated from measurements performed in the dry and wet season over the city of São Paulo.

## 2. Methodology

The lidar in São Paulo [Município de São Paulo (msp) lidar] is a single-wavelength backscatter system pointing vertically to the zenith and operating in the coaxial mode. The light source is based on a commercial Nd:YAG laser (Brilliant, Quantel SA) operating at the second harmonic frequency (SHF), namely at 532 nm, with a fixed repetition rate of 20 Hz. The average emitted power can be selected up to values as high as 3.3 W. The emitted laser pulses have a divergence of less than 0.5 mrad. A 30-cm-diameter telescope (focal length  $f = 1.3$  m) is used to collect the backscattered laser light. The telescope field of view (FOV) is variable (0.5–5 mrad) by using a small diaphragm. The lidar is currently used with a fixed FOV of the order of 1 mrad, which according to geometrical calculations permits a full overlap between the telescope FOV and the laser beam at heights higher than 300 m above the lidar system.

As stated before, collocated Cimel aerosol measurements were performed to determine the AOT values at several wavelengths in the visible spectrum and thus, to enable the assessment of the AE values at the same spectral region. The principle of operation of the Cimel instrument is to acquire aureole and sky radiance measurements. The standard measurements are taken 15 min apart to allow for cloud contamination checking. These measurements are taken in the whole spectral interval (440–870 nm), and their number depends on the daytime duration. The instrument precision and accuracy follow the standard Langley plot method within the standards employed by AERONET (Holben et al. 1998). The Cimel sun photometer is calibrated periodically by a remote computer or locally under the supervision of AERONET. The calibration methodology assures coefficient accuracy between 1% and 3%; nonetheless, various instrumental, calibration, atmospheric, and methodological factors influence the precision and accuracy of optical thickness and effectively the total uncertainty in the AOT retrieved values is less than 8% (Landulfo et al. 2003).

### a. Lidar data retrieval

In general, the inversion of the lidar profile is based on the solution of the basic lidar equation, taking into account the atmospheric solar background radiation correction (Papayannis and Chourdakis 2002). The re-

retrieval of the aerosol optical properties is based on the measurements of the aerosol backscatter coefficient  $\beta_{\text{aer}}$  at 532 nm, up to an altitude of 5–6 km. The determination of the vertical profile of the aerosol backscatter coefficient relies on the lidar inversion technique following a modified Klett’s algorithm (Klett 1985; Grabowski and Papayannis 1999). One has, however, to bear in mind that this inversion technique is an ill-posed problem in the mathematical sense, leading to errors as large as 30% when applied (Papayannis and Chourdakis 2002). In general, the inversion of the lidar profile is based on the solution of the lidar Eq. (1), under the assumption of the single scattering approximation:

$$P(\lambda, R) = P_L \left( \frac{c\tau}{2} \right) \beta(\lambda, R) A_0 \xi(\lambda) \zeta R^{-2} \times \exp \left[ -2 \int_0^r \alpha(\lambda, r) dr \right], \quad (1)$$

where  $P(\lambda, R)$  is the lidar signal received from a distance  $R$  at the wavelength,  $P_L$  is the emitted laser power,  $A_0$  is the telescope receiving area,  $\xi(\lambda)$  is the receiver’s spectral transmission factor,  $\beta(\lambda, R)$  is the atmospheric volume backscatter coefficient,  $\zeta(R)$  is the overlap factor between the field of view of the telescope and the laser beam,  $\alpha(\lambda, R)$  is the extinction coefficient,  $c$  is the light speed, and  $\tau$  is the laser pulse length.

To make the lidar equation solvable it is necessary to establish a relation between  $\alpha(\lambda, R)$  and  $\beta(\lambda, R)$ . This is achieved assuming the lidar ratio, or extinction-to-backscatter ratio, relationship. However, it is known that the LR depends on several physical–chemical parameters inherent to the aerosols being inspected, such as the aerosol refractive index and size and shape distribution of the aerosols particles (Bösenberg et al. 1997). To derive the appropriate “correct” values of the vertical profile of aerosol backscatter coefficient in the lower troposphere we used an iterative inversion approach (by “tuning” the LR values) based on the intercomparison of the AOT values derived by lidar and Cimel data (Landulfo et al. 2003, 2004), assuming the absence of stratospheric aerosols and that the PBL is homogeneously mixed between ground and 300-m height, where the lidar overlap factor is close to 1. Once the correct values of the vertical profile of the aerosol backscatter coefficient were derived (when the difference between the AOTs derived by Cimel and lidar was less than 10%) we reapplied Klett’s inversion technique (Klett 1981, 1985), using the appropriate LR values, to retrieve the final values of the vertical profiles of the backscatter and extinction coefficient at 532 nm. The LR obtained from the Cimel database was used as well,

according to the following expression (Dubovik et al. 2006):

$$S_i = \frac{4\pi}{\omega_0 P_i(180)}, \quad (2)$$

where  $\omega_0$  is the single scattering albedo (SSA) and  $P_i(180)$  is the backscattering phase function (PF).

*b. Sun photometer data retrieval*

The inversion of the solar radiances measured by the Cimel sun photometer to retrieve the AOT values is based on the Beer–Lambert law, assuming that the contribution of multiple scattering within the small field of view of the sun photometer is negligible:

$$I_\lambda = I_\lambda^0 \exp \left( -\frac{\tau_\lambda}{\mu_s} \right), \quad (3)$$

where  $I_\lambda$  and  $I_\lambda^0$  are the solar irradiances at the top of the atmosphere and at ground level, respectively, and  $\mu_s$  is the cosine of the solar zenith angle;  $\tau_\lambda$  is the total atmospheric optical thickness from the Rayleigh and aerosol contributions, as well the ozone and water vapor absorption at 670 and 870 nm, respectively. The molecular (Rayleigh) scattering contribution is taken into account to retrieve the aerosol optical thickness values at 532 nm, determined by the relation

$$\frac{\tau_{532}^{\text{aer}}}{\tau_{500}^{\text{aer}}} = \left( \frac{532}{500} \right)^{-\text{AE}}, \quad (4)$$

where the AE value (Ångström 1964) was derived from the measured optical thickness in the blue and red channels (440 and 670 nm):

$$\text{AE} = - \frac{\log \left( \frac{\tau_{440}^{\text{aer}}}{\tau_{670}^{\text{aer}}} \right)}{\log \left( \frac{440}{670} \right)}. \quad (5)$$

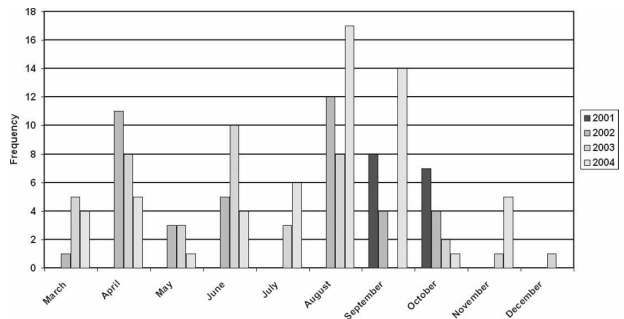


FIG. 1. Temporal display of measurements taken by the lidar station at São Paulo over the years 2001–04.

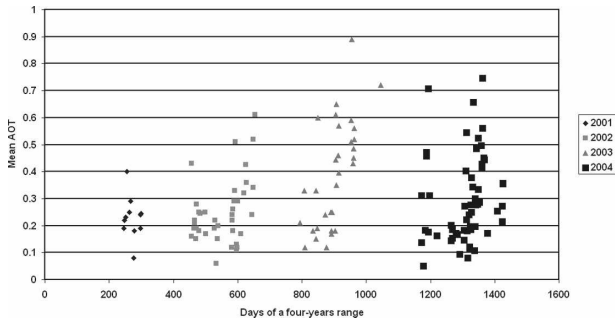


FIG. 2. Daily average AOT at 532 nm for the period 2001–04, when both the lidar station and sun photometer were operational.

3. Results and discussion

The lidar and sun photometer data were acquired in a 4-yr period (1 January 2001 up to 31 December 2004). In Fig. 1 we present the number of days per month, where lidar data were obtained for the whole period of observations. From this figure one can realize that most of the lidar measurements have been obtained in the so-called dry season when the atmospheric pollutant dispersion is worse and the air quality in the city reaches its critical values. Among these data, we have selected only those for which simultaneous Cimel data are also available. Figure 2 shows the daily mean AOT values obtained by lidar at 532 nm for the 4-yr period. We see that the mean AOT values span from 0.05 to 0.9. An increasing trend of the AOT values is clearly visible in the lidar data, as well as in the relative Cimel data showing the mean LR values (Fig. 3), from which it would be very premature to take any conclusions at present. However, if the increasing trend was related to local air pollution sources, one should also find increasing trends of suspended particles over the city, which is not the case according to locally available data (not shown).

In Fig. 3 we can certainly see peaks over 140 sr, in-

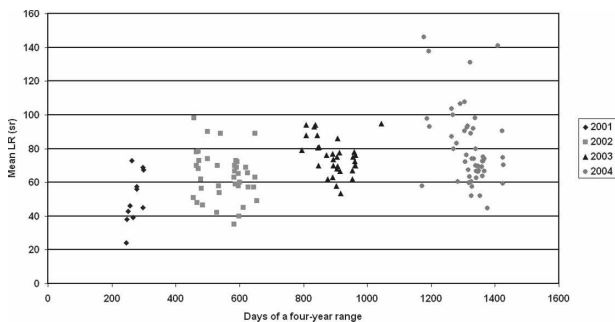


FIG. 3. Daily average Cimel LR at 532 nm for the period 2001–04, when both the lidar station and sun photometer were operational.

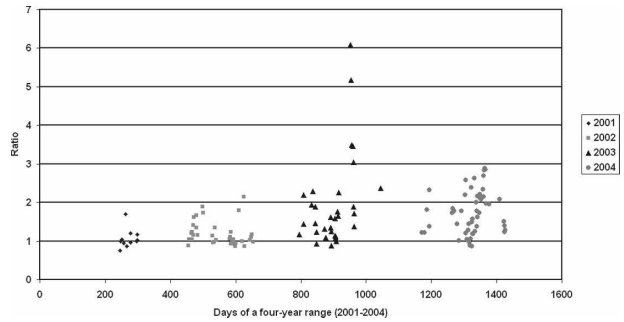


FIG. 4. Cimel LR for the period 2001–04, when both the lidar station and sun photometer were operational.

dicating aerosol with strong absorption. However, the most plausible reason for this enhancement in the LR would be due to the fact that calculations carried in the process take a spherical aerosol distribution (Cattrall et al. 2005). Using the LR values retrieved from the lidar data by the “tuning method” described above, we show in Fig. 4 the ratio between the LRs retrieved by the two methods, in which one sees that there is an average of about 1.8 larger values when using the Cimel LRs in comparison with the ones retrieved by the lidar. One can observe, though, some cases in which those ratios are larger than 5. Those LR values when normalized to the lidar ones (Cimel LRs divided by 1.8) still suggest a larger extinction over backscatter that can at first sight indicate the presence of biomass burning aerosols that can reach the city of São Paulo in some instances (Lan-dulfo et al. 2003).

The other aspect we wished to examine was a possible seasonal signature in aerosol properties over São Paulo, since we highlight in this part of the country two different seasons: the wet season spanning from March until June and the dry season between July and November. For that reason we have separated the measured LR mean values for these two seasons and the respective results are shown in Fig. 5. Thus, we see that

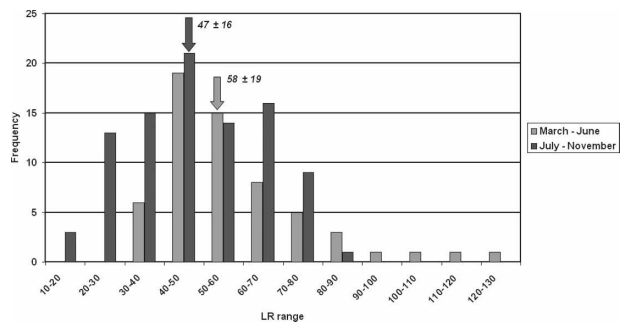


FIG. 5. Seasonal Cimel LR distribution between the dry and wet season for the 2001–04 period.

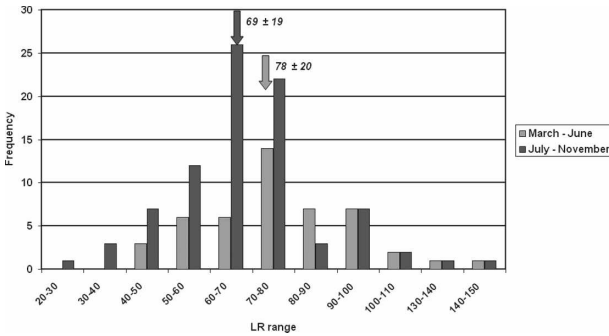


FIG. 6. Seasonal LR distribution between the dry and wet season for the 2001–04 period.

there are, in general, larger LR values ( $58 \pm 19$  sr) during the wet season, when compared to the ones obtained during the dry period ( $47 \pm 16$  sr), although, the frequency counts are higher during the dry season. The uncertainties shown here are those obtained from the Gaussian fitting of the data, while during the iteration explained above they are about 10%–15% of the individual LR obtained. However, our data are not statistically significant, so definite conclusions cannot be drawn for the moment. The dry season LR distribution shows a nearly Gaussian distribution, around the LR value of 40–50 sr, while the wet season LR distribution deviates more from the Gaussian distribution, with a central LR value of 50–60 sr. These findings, in any case, show that during the wet season the LR values are greater, which indicates that larger absorption by the aerosols takes place during this period.

Evaluating the Cimel LR seasonal distribution (Fig. 6) we find a similar behavior, as before, and that the mean LR values are on the order of  $78 \pm 20$  sr on the wet season and about  $69 \pm 19$  sr in the dry season, although the frequency counts are more important during the dry season. This trend is observed in the AOT

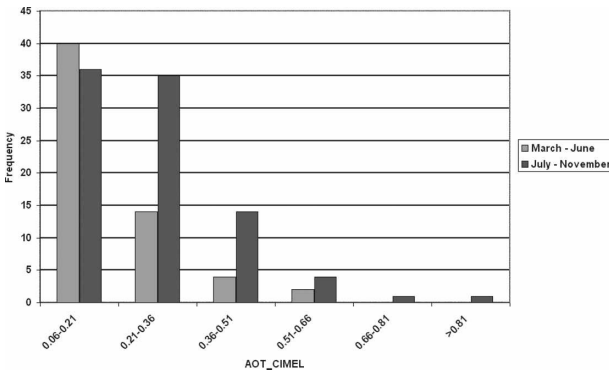


FIG. 7. Seasonal lidar AOT at 532 nm in the dry (July–November) and wet (March–June) season for the 2001–04 period.

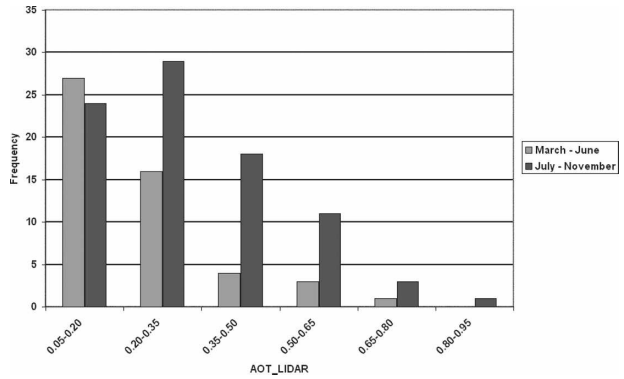


FIG. 8. Seasonal Cimel AOT at 532 nm in the dry (July–November) and wet (March–June) season for the 2001–04 period.

distribution shown in Fig. 7, as one can see that the smaller values are more concentrated in the wet period than in the dry season, thus highlighting the better air quality in that period. A similar behavior is shown in Fig. 8, concerning the AOT values at 532 nm, where again the dry season presents the higher frequency counts.

Regarding the seasonal distribution of the Ångström exponent values evaluated from the Cimel data (Fig. 9), we see that most of the AE values range between 1.3 and 2 for both periods (wet and dry), which means that mostly fine particles (related to anthropogenic activities) are found above our measuring site, following a bimodal frequency distribution. Figure 10 shows the AE versus LR values from the Cimel measurements during the 2001–04 period. In this figure we can see that in general, most of the AE values are between 1.3 and 1.9, thus indicating the presence of rather small particles, having LR values mostly between 40 and 100 sr. We also find a tendency in the larger particles (AE < 1.2) to present higher LR values (LR > 60 sr) and thus show a higher absorption, which might result from the

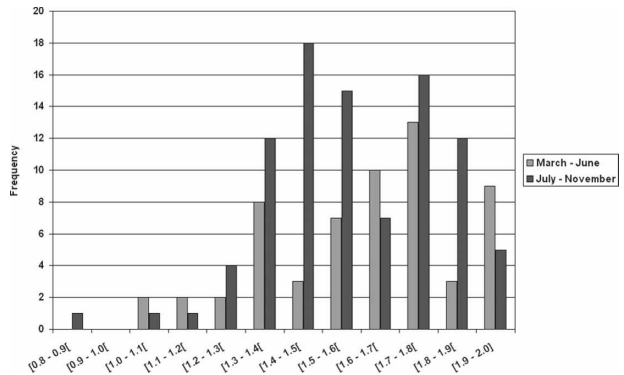


FIG. 9. The Ångström exponent seasonal distribution.

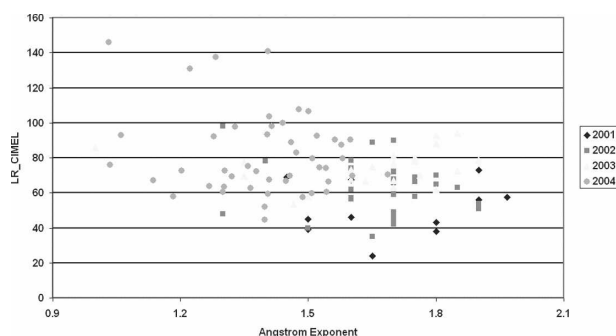


FIG. 10. AE vs LR values from Cimel measurements during the 2001–04 period.

mixture of anthropogenic and biomass burning aerosol particles.

#### 4. Conclusions

In this paper we examined the seasonal distribution of the AOT, LR, and AE values, as well as the correlation between AE and LR values derived by lidar and sun photometer data. The analysis of these data showed an important trend in the seasonal signature of the LR indicating a change of the predominant type of aerosol between the dry and wet seasons. Thus, during the wet season, the LR values are greater (50–60 sr), which indicates that larger absorption by the aerosols takes place during this period. The corresponding AE values range between 1.3 and 2 for both periods, which means that mostly fine particles (related to anthropogenic activities) are found above our measuring site, following a bimodal frequency distribution. This trend is observed in the AOT distribution, as the smaller values are more concentrated in the wet period than in the dry season, thus highlighting the better air quality in that period. A tendency was also found regarding the larger particles ( $AE < 1.2$ )—measured mostly during 2004—that presented higher LR values ( $LR > 60$  sr) and thus showed a higher absorption, which might result from the mixture of anthropogenic and biomass burning aerosol particles.

**Acknowledgments.** The authors would like to express their gratitude to the AERONET team members for providing the data in their sites, in particular to the local data manager, Dr. Paulo Artaxo. Also we thank the funding agencies FAPESP (Fundação de Amparo à

Pesquisas do Estado de São Paulo), CNPq (Conselho Nacional de Pesquisas) e CAPES for supporting projects and scholarships for the past five years.

#### REFERENCES

- Ackermann, J., 1998: The extinction-to-backscatter ratio of tropospheric aerosol: A numerical study. *J. Atmos. Oceanic Technol.*, **15**, 1043–1050.
- Anderson, T. L., S. J. Masonis, D. S. Covert, R. J. Charlson, and M. J. Rood, 2000: In situ measurements of the aerosol extinction-to-backscatter ratio at a polluted continental site. *J. Geophys. Res.*, **105** (D22), 26 907–26 915.
- Angström, A., 1964: The parameters of atmospheric turbidity. *Tellus*, **16**, 64–75.
- Bösenberg, J., R. Timm, and V. Wulfmeyer, 1997: Study of retrieval algorithms for a backscatter lidar. MPI Final Rep. 226, Hamburg, Germany, 66 pp.
- Cattrell, C., J. Reagan, K. Thome, and O. Dubovik, 2005: Variability of aerosol and spectral lidar and backscatter and extinction ratios of key aerosol types derived from selected Aerosol Robotic Network locations. *J. Geophys. Res.*, **110**, D10S11, doi:10.1029/2004JD005124.
- Clemesha, B. R., and S. N. Rodrigues, 1971: Stratospheric scattering profile at 23 degrees south. *J. Atmos. Terr. Phys.*, **33**, 1119–1125.
- Dubovik, O., and Coauthors, 2006: Application of spheroid models to account for aerosol particle nonsphericity in remote sensing of desert dust. *J. Geophys. Res.*, **111**, D11208, doi:10.1029/2005JD006619.
- Grabowski, J., and A. Papayannis, 1999: Lidar inversion algorithm for the simultaneous retrieval of the vertical profile of the aerosol extinction and backscattering coefficients in the troposphere. *Environmental Sensing and Applications*, M. R. Carleer et al., Eds., International Society for Optical Engineering (SPIE Proceedings, Vol. 3821), 12–18.
- Holben, B., and Coauthors, 1998: Aeronet—a federal instrument network and data archive for aerosol characterization. *Remote Sens. Environ.*, **66**, 1–16.
- Klett, J. D., 1981: Stable analytical inversion solution for processing lidar returns. *Appl. Opt.*, **20**, 211–220.
- , 1985: Lidar inversion with variable backscatter/extinction ratios. *Appl. Opt.*, **24**, 1638–1643.
- Landulfo, E., and Coauthors, 2003: Synergetic measurements of aerosols over São Paulo, Brazil using LIDAR, sunphotometer and satellite data during the dry season. *Atmos. Chem. Phys.*, **3**, 1523–1539.
- , A. Papayannis, R. F. Souza, and A. Z. Freitas, 2004: Lidar aerosol profile categorisation in São Paulo, Brazil. *Reviewed and Revised Papers Presented at the 22nd International Laser Radar Conference*, Vol. 1, G. Pappalardo and A. Amodeo, Eds., ESA Publications Division, 499–502.
- Papayannis, A., and G. Chourdakis, 2002: The EOLE project. *Int. J. Remote Sens.*, **23**, 179–196.
- Takamura, T., Y. Sasano, and T. Hayasaka, 1994: Tropospheric aerosol optical properties derived from lidar, sun photometer, and optical particle counter measurements. *Appl. Opt.*, **33**, 7132–7140.